J Supercond Nov Magn (2017) 30:2603–2608
DOI 10.1007/s10948-017-4082-9

ORIGINAL PAPER

Role of the Dipolar Interaction in Single-Walled Ferromagnetic Nanotubes: Monte Carlo Study

H. D. Aristizabal[1] · H. Barco-Rios[1] · E. Restrepo-Parra[1]

Received: 14 March 2017 / Accepted: 20 March 2017 / Published online: 31 March 2017

Abstract This document presents a study of the influence of the dipolar interactions and geometrical parameters on the magnetic properties of single-walled ferromagnetic nanotubes built by using square and hexagonal unit cells. For this study, a Hamiltonian, which includes dipolar interactions and nearest neighbor classical Heisenberg model, was used; furthermore, the Monte Carlo method combined with the Metropolis algorithm was used to determine the observables required. The analyses were focused on the magnetization per magnetic site and the critical temperature that was obtained by using specific heat peaks. These properties were calculated varying the length, diameter, boundary conditions, dipolar parameter and unit cell type. It was observed that the system showed different behaviors depending on the use of periodic or free boundary conditions; moreover, there is a strong influence of the unit cell type on the magnetic properties, caused by the difference of the number coordination between them. For both cases, square and hexagonal unit cells, the critical temperature increased as the nanotube length was increased; nevertheless, the diameter produced an inverse effect. On the other hand, the dipolar interaction always generated an increase in the critical temperature. This behavior allows us to conclude that longrange dipolar interactions have a strong effect on the magnetic properties of the single-walled magnetic nanotubes.

Keywords Exchange coupling · Long-range dipolar interaction · Monte Carlo simulations · Heisenberg

Academic Discipline and Sub-disciplines

Computational Physics

✉ H.D. Aristizabal
hdaristizabals@unal.edu.co

[1] PCM Computational Applications, Universidad Nacional de Colombia-Sede Manizales, A.A. 127, Manizales, Colombia

1 Introduction

Magnetic nanotubes as well as nanotube arrays and combining attractive tubular structures with tuneable magnetic properties are promising candidates for potential applications in a broad range of nanotechnological areas such as high-density data storage, nanoelectromechanical devices, as well as biotechnology like medicine delivery, biosensors, and chemical and biochemical separations [1–8].

Among these new nanomaterials, the nanotubes, in contrast to solid wires, have inner voids that reduce the density of materials and make them easier to float in solutions, a desirable property in biotechnology [9]. The inner hollow itself can be used to capture large biomolecules [10]. Besides, as magnetic materials, they are free of vortex cores, which make the vortex state more stable than the one from nanowires. This makes nanotubes more suitable as candidates for computer elements of memory and as a tool to create superconductors with high critical fields [11].

Recently, there have been simulations that showed the behavior of nanowires and magnetic nanotubes, in which different properties were studied. Bin-Zhou et al. [12] studied transversal and longitudinal magnetic correlations (TMC, LMC) of squared ferromagnetic nanotubes; the results of this research revealed that magnetic correlation

varies according to the orientation of the correlation. Kaneyoshi [13] showed the dependence of temperature in the total magnetization of two systems (nanotubes and nanowires); the results showed significant differences between nanotubes and nanowires due to their core structures. Salinas et al. [14] studied the magnetic properties of single-walled nanocylinders with zig-zag edges. The results of this research showed that there exists a strong dependence between critical temperature and dipolar interaction. The studies that have been carried out on simulations of ferromagnetic cylindrical systems, which study different properties, do not focus on the effect produced by the dipolar interactions when the parameters like crystalline structure, length, and diameter change.

According to our results, the parameter (γ) included in the Hamiltonian has a strong influence on critical temperature. Despite the fact that dipolar energy between the two spins is much weaker for the interaction exchange, it has an important role on the magnetic behavior of the system, allowing a better approximation of the energy calculation. To understand the ferromagnetic behavior of the SWMNs, the dependence on the temperature was calculated, including the influence of the dipolar interaction, magnetic properties as magnetization, susceptibility, and specific heat [15]. For this study, two types of structures formed by square magnetic nanotube (SMNT) and hexagonal magnetic nanotube (HMNT) unit cells were considered (as shown in Fig. 1a, b). Previously [15], a similar system containing two identical ferromagnetic nanotubes were studied, although dipolar coupling was not considered. The main goal of this study is to analyze the influence of the dipolar interaction on the calculation of the critical temperature for the SMNT and the HMNT unit cell geometries.

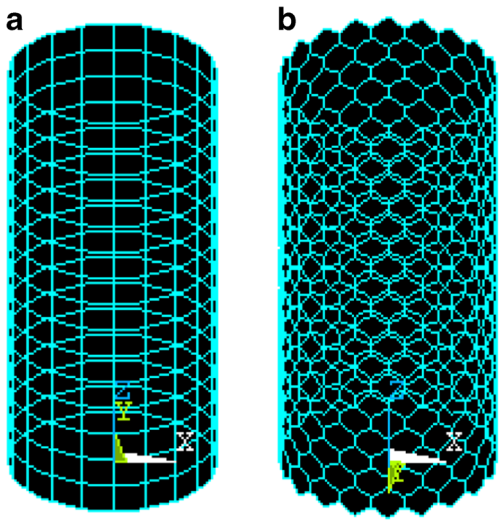

Fig. 1 Schemes of (**a**) a square magnetic nanotube (SMNT) and (**b**) a hexagonal magnetic nanotube (HMNT)

2 Method Description

The Hamiltonian of the model considered in this work is defined as

$$H = -J \sum_{<i,j>} \vec{S}_i \vec{S}_j - K \sum_i \left(\vec{S}_i . \hat{n}_i\right)^2 + \delta \sum_{<i,j>} \times \left[\frac{\vec{S}_i . \vec{S}_j}{r_{ij}^3} - 3 \frac{\left(\vec{S}_i . \vec{r}_{ij}\right)\left(\vec{S}_j . \vec{r}_{ij}\right)}{r_{ij}^5} \right] \quad (1)$$

This model is suitable for nanotubes because all the calculations depend on the atomic interactions. $\vec{S}_i$ and $\vec{S}_j$ are the unitary classical spins of the nearest neighboring atoms (with magnitude $S = 1$). The first term represents the exchange energy (short-range interaction), assumed to be $J = 1.0$meV as an arbitrary value for the integral exchange. The second term refers to the magnetocrystalline anisotropy, defined as a constant $K = 1$meV/spin and $\hat{n}_i$ is a vector unit providing the axis direction which was assumed to be the longitudinal direction of the nanotube. The last term represents the dipolar energy, accounting for longrange interactions. Here, r_{ij} is the relative distance between atoms i and j and $\delta = 0.5$meV represents the dipolar parameter. Competition between short and long-range interactions is determined by the ratio $\gamma = \delta/J$, which is considered to range between 0 and 1 [14]. Two values $\gamma = 0.0$ and 0.5 were assumed based on the fact that the dipolar interaction is usually one or two orders of magnitude less than the exchange interaction In the ground state of the system each nanotube behaves as a single domain, with spins pointing in the same direction. The dipolar interaction increases the energy of the system and the ground state is ferromagnetic, with the total magnetic moments of the nanotube longitudinally oriented with the tube even if the nanotube is too long We employed Monte Carlo simulations for the two singlewalled ferromagnetic nanotubes through the use of the Metropolis algorithm [16, 17]. For each Monte Carlo step (MCs) random trials were performed to change the spins of the ferromagnetic nanotube. The procedure we used to determine the equilibrium states of the system is based on the minimization of free energy. In each trial, a given spin is selected randomly, and we attempt to move it to a new position in a way that the deviation from the old state is random, but within a maximum solid angle. Then, we calculate the energy's system change (ΔE). If $\Delta E \leq 0$, the transition to a different configuration is accepted. However, if $\Delta E > 0$, the transition to a different configuration is made based on the probability exp $(-\Delta E/KbT)$. To determine the average magnetic properties, we considered 2.0×10^4 Monte Carlo steps (MCS_{max}), where the first $1.0\times10^4(N)$ was discarded due to the thermalization process. We calculated the average magnetization and its components in the x, y, and z

directions as functions of the temperature. First we obtained the magnetization and magnitude susceptibilities for each ith Monte Carlo step, carrying out a scan over the N ion samples; then the average values of these observables were obtained over the Monte Carlo steps for each temperature [18]. The average magnetization was calculated using the next expression:

$$\langle |m_t| \rangle = \frac{1}{N(\mathrm{MCS}_{\max} - N_{\mathrm{o}})} \sum_{i+N_0}^{\mathrm{MCS}_{\max}} \left(\vec{M}_i . \vec{M}_i \right)^{1/2} \tag{2}$$

$$\vec{M}_i \vec{M}_i = M_i^2 = \left[\left(\sum_{j=1}^{N} S_j^x \right)^2 + \left(\sum_{j=1}^{N} S_j^y \right)^2 + \left(\sum_{j=1}^{N} S_j^z \right)^2 \right]_i \tag{3}$$

where s_j^x, s_j^y and s_j^z are the spin components in the x, y and z directions respectively for the jth magnetic ion; for the construction of the samples atoms were arranged in a rolled-up simple square or a hexagon. Panels a and b of Fig. 1 show both geometries for single-walled SMNTs and HMNTs respectively. The nomenclature for interatomic distance is taken from a previous paper [17] To compute the error was generated 10 simulations per point and we use the susceptibility to determinate the average of the critical temperature. Finally, the diameter was calculated using the next expression [15]:

$$m = \left(\frac{\pi}{c} \right) d \tag{4}$$

where d = diameter c = lattice parameter, and m = maxim number of atoms per ring.

3 Results and Analysis

As stated, different values for the dipolar parameters between all spin pairs were assumed to reach the system's ground state. Figures 2 and 3 show the critical temperature $T_C(K)$ as a function of the length L for two different values of the γ parameter $\gamma = 0.0$ and $\gamma = 0.5$ for square (SMNTs) and hexagonal (HMNTs) lattices, with non and with periodic boundary conditions (NPBC) (PBC). Different samples in 15 sizes, from $L = 2$ to $L = 16$Å, were examined. Bigger samples were not implemented because at $L > 16$Å properties stop changing significantly. Figure 2 shows that T_C is higher for the SMNTs than the HMNTs; this is attributed to a greater coordination number (CN). For SMNTs, CN = 4, whereas for the HMNTs, CN = 3. A larger number of bonds per atom produce better atomic cohesiveness, meaning that the atom with CN = 4 is embedded in a greater electronic density [19]. For this reason, SMNTs exhibit critical higher temperatures than the HMNTs, as shown in Figs. 2 and 3. The curves presented in Fig. 3 (PBC) show similar behavior to those presented in Fig. 2 (NPBC); the difference seen in Fig. 3 is that the thermal component produces a greater T_C than the one observed in Fig. 2. A system with nonperiodic boundary conditions (NPBC) makes an imperfect surface where there is no interaction; this means that inside the SMNTs and HMNTs with NPBCs (see Fig. 2), the cohesive energy is stronger than in the borders. This behavior is caused by the lower CN within the limits of the structure. If we observe all the atoms in the limits of the structure, we can see a system that must be considered ferromagnetic. If the cohesive energy is directly determined by the bond's product and its unit energy

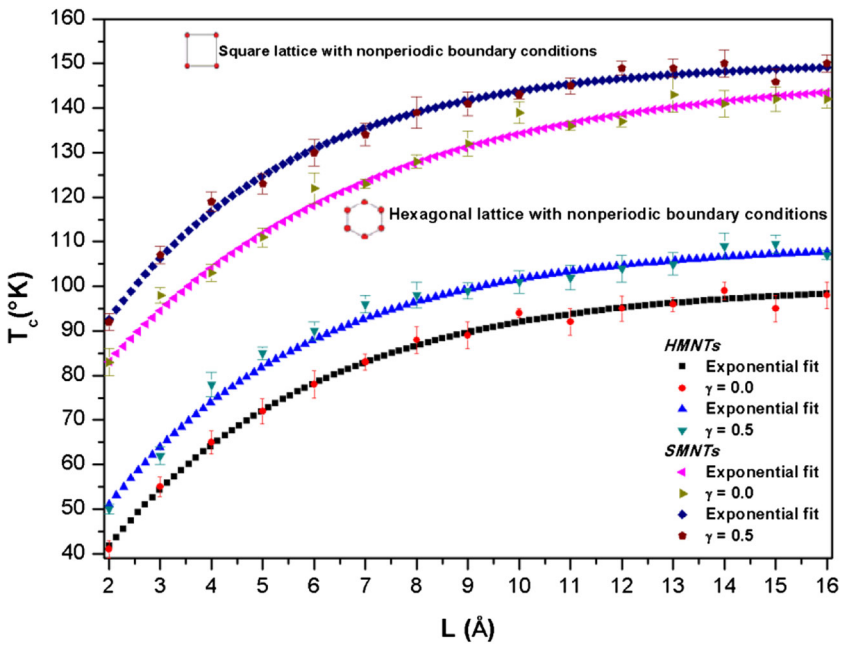

Fig. 2 Critical temperature T_c as a function of the length L for two values of γ parameter $\gamma =$ and $\gamma = 0.5$ for SMNTs and HMNTs with non-periodic boundary conditions and constant diameter $D \approx$ 5Å

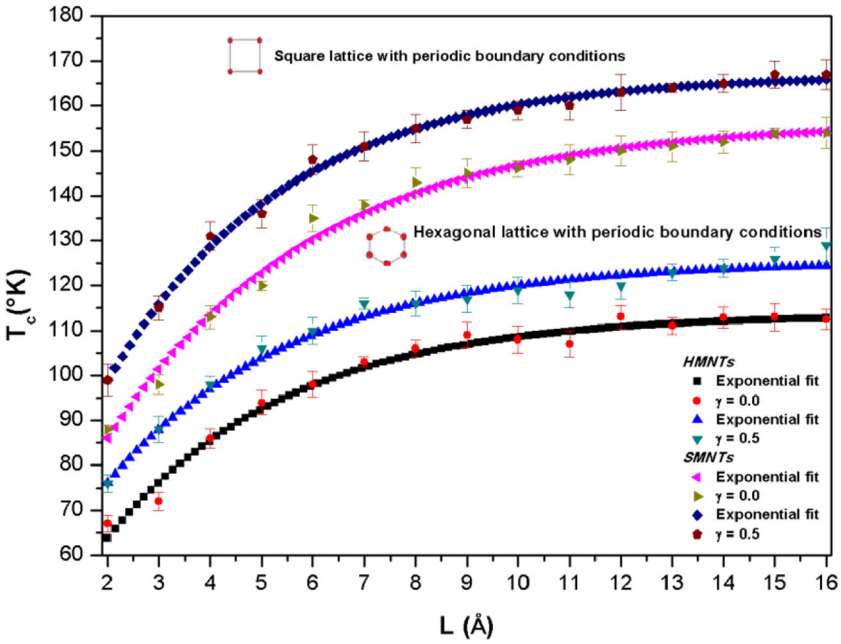

Fig. 3 Critical temperature T_C as a function of the length L for two values of γ parameter $\gamma = 0.0$ and $\gamma = 0.5$ for SMNTs and HMNTs with periodic boundary conditions and constant diameter $D \approx 5$Å

[20–23], SMNT and HMNT with (PBC) (see Fig. 3) do not exhibit surface effects and the cohesive energy is the same for all the atoms in the entire nanotube, causing the system to show a higher T_C. However it was found that the magnetic behavior of the nanotubes could be strongly modified because of the length (Figs. 2 and 3). This can be attributed to the magnetic bond density (MBD). When the SWFNs increase their length, the coupling energy (CE) increases with the number of atoms. Moreover, Figs. 2 and 3 show the behavior of the T_C with and without the long-range dipolar interaction. The dipolar parameter δ determined by Hamiltonian shows a significant increase in the T_C for the SMNTs and HMNTs. If $\delta = 0.0$meV, the γ parameter is not considered in the simulation and the thermalization process is considered with non-dipolar energy. However, when $\delta = 0.5$meV, it is assumed that the Hamiltonian of the long-range dipolar interactions increases significantly the Curie temperature for both the PBC and NPBC systems. Figures 4 and 5 show the critical temperature $T_C$as a function of the diameter D for two values of γ parameter $\gamma =$ and $\gamma = 0.5$ for SMNT and HMNT lattices with and without periodic boundary conditions. Several samples possessing 11 diameters, from $D \approx 5$, 6, 7, 8, 9, 10, 11, 12, 13, 14, and 15 Å were examined. Figures 4 and 5 show that there is

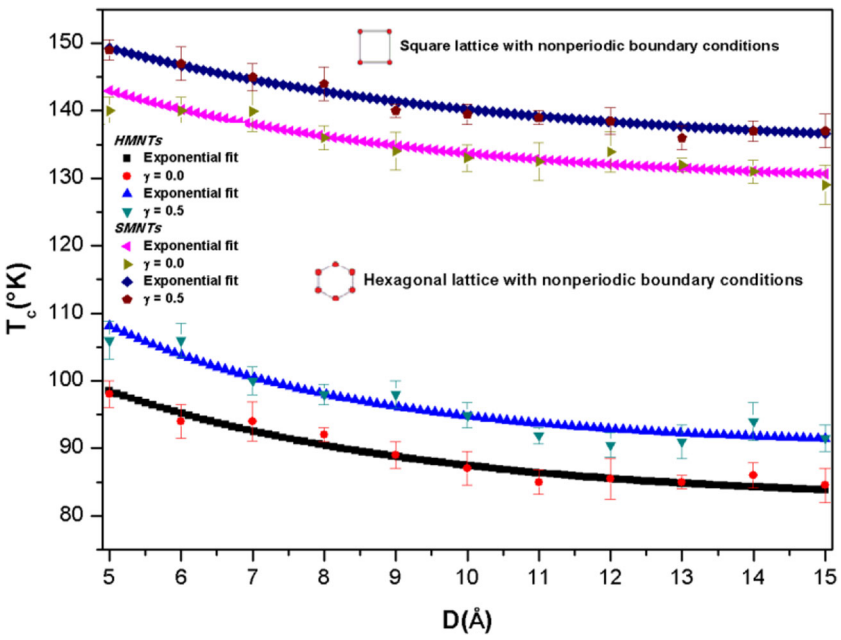

Fig. 4 Critical temperature T_C as a function of the diameter D for two values of γ parameter $\gamma = 0.0$ and $\gamma = 0.5$ for SMNTs and HMNTs with non-periodic boundary conditions and constant length $L = 16$Å

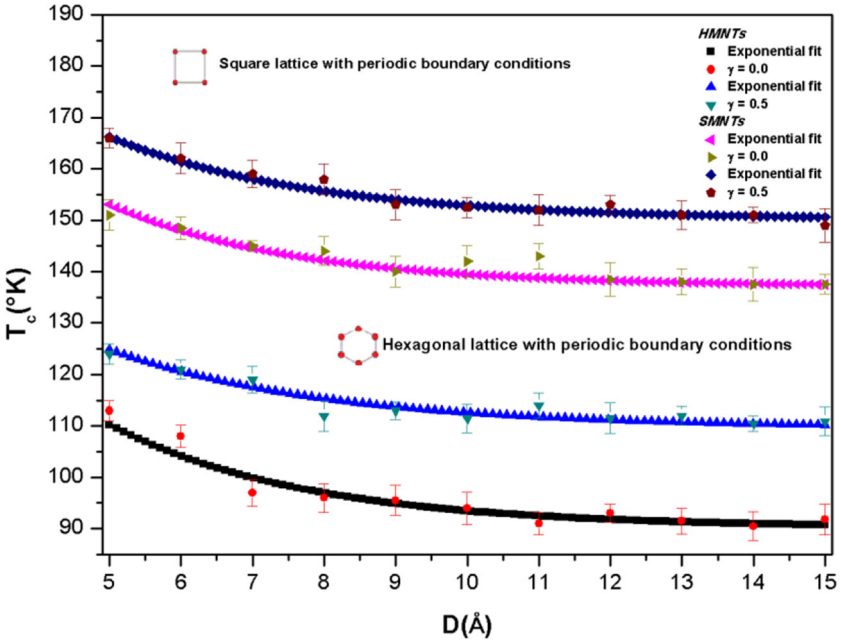

Fig. 5 Critical temperature T_c as a function of the diameter D for two values of γ parameter $\gamma = 0.0$ and $\gamma = 0.5$ for SMNTs and HMNTs with periodic boundary conditions and constant length $L = 16$Å

a decrease in T_C as the nanotube diameters increase. This behavior is attributed to MBD. When the diameter of the SWFNs increase, the coupling energy (CE) decreases since the distance between them increases and it is much more difficult for the atoms to interact with their neighbors. An increase in the inter-atomic distance will cause the system to go to a less cohesive energy state. Finally, we observe similar behaviors in the SMNTs and HMNTs presented in Figs. 2 and 3 with the T_C shown in Figs. 4 and 5. The effects produced by the CN and boundary conditions (BC) are the same, with the difference that a diameter increase produces magnetic disorders that result in a decrease of T_C for the system [24–27].

4 Conclusions

In this study, Monte Carlo simulations of magnetic nanotubes with two different unit cells (square and hexagonal) were conducted. We observed that some magnetic and thermodynamic properties of these structures exhibit a strong dependence in long-range dipolar interactions. It is important to mention that dipole-dipole interactions can induce long-range ferromagnetic order in an infinitely extended, isotropic, three-dimensional Heisenberg ferromagnet. As the γ parameter increases, the critical temperature also increases, causing the system to go to a higher thermodynamic state. Furthermore, a noticeable dependence of these properties on the length and diameter of the SWFNs was observed. The general conclusion from our investigation is that the simulations performed using long-range dipolar interactions result in a better approximation of the magnetic behavior in the SWFNs. Finally, we observed that the critical temperatures can be strongly modified because of the geometry of the nanotubes. However, the dipolar parameter modified the behavior of the T_C by a couple of degrees, which may be very important in biomedical and data storage simulations.

Acknowledgments The authors gratefully acknowledge the financial support of the Dirección Nacional de Investigación of the Universidad Nacional de Colombia during the course of this research under project 20101007903—entitled The Theoretical Study of Physical Properties of Hard Materials for Technological Applications.

References

1. Chen, A.P., González, J., Guslienko, K.Y.: J. Appl. Phys. **109**, 073923 (2011)
2. Sui, Y.C., Skomski, R., Sorge, K.D., Sellmyer, D.J.: Appl. Phys. Lett. **84**, 1525 (2004)
3. Hou, S., Harell, C., Trofn, L., Kohli, P., Martin, C.R.: J. Am. Chem. Soc. **126**, 5674 (2004)
4. Nielsch, K., Castaño, F.J., Ross, C.A., Krishnan, R.: J. Appl. Phys. **98**, 034318 (2005)
5. Son, S.J., Reichel, J., He, B., Schuchman, M., Lee, S.B.: J. Am. Chem Soc. **127**, 7316 (2005)
6. Wang, Z.K., Lim, H.S., Liu, H.Y., Ng, S.C., Kuok, M.H., Tay, L.L., Lockwood, D.J., Cottam, M.G., Hobbs, K.L., Larson, P.R., Keay, J.C., Lian, G.D., Johnson, M.B.: Phys. Rev. Lett. **94**, 137208 (2005)
7. Daub, M., Knez, M., Goesele, U., Nielsch, K.: J. Appl. Phys. **101**, 09J111 (2007)
8. Han, X.F., Wen, Z.C., Wei, H.X.: J. Appl. Phys. **103**, 07E933 (2008)
9. Landeros, P., Suarez, O.J., Cuchillo, A., Vargas, P.: Phys. Rev. B **79**, 024404 (2009)

10. Son, S.J., Reichel, J., He, B., Schuchman, M., Lee, S.B.: J. Am. Chem. Soc **127**, 7316 (2005)
11. Sun, C., Pokrovsky, V.L.: J. Magn. Magn. Mater. **355**, 121–130 (2014)
12. Mi, B.Z., Wang, H.Y.: J. Magn. Magn. Mater. **390**, 132–136 (2015)
13. Kaneyoshi, T.: J. Magn. Magn. Mater., 1–19 (2016)
14. Salinas, H.D., Restrepo, J.: J. Supercond. Nov. Magn. **25**, 2217–2221 (2012)
15. Salazar-Enríquez, C.D., Restrepo-Parra, E., Restrepo, J.: J. Magn. Magn. Mater. **324**, 1631–1636 (2012)
16. Konstantinova, E., Sales, J.A.: J. Magn. Magn. Mater. **367**, 86–91 (2014)
17. Verdier, P., Ledue, D., Patte, R.: J. Magn. Magn. Mater. **271**, 355–363 (2004)
18. Masrour, R., Bahmad, L., Hamedoun, M., Benyoussef, A., Hlil, E.K.: Phys. Lett. A **378**, 276–279 (2014)
19. Daw, M.S., Baskes, M.I.: Phys. Rev. B **29**, 6443–6453 (1983)
20. Xie, D., Wang, M.P., Qiw, H.: J. Phys.: Condens. Matter. **16**, L401–L405 (2004)
21. Cao, L.F., Xu, G.Y., Xie, D., Guo, M.X., Luo, L., Li, Z., Wang, M.P.: Phys. Status. Solidi. B **243**, 2745–2755 (2006)
22. Sun, C.Q., Tay, B.K., Zeng, X.T., Li, S., Chen, T.P., Zhou, J., Bai, H.L., Jiang, E.Y.: J. Phys.: Condens. Matter. **14**, 7781–7795 (2002)
23. Xie, D., hong, Q.W., Wang, M.P.: Acta Metall. Sinica **41**(5), 458–462 (2004)
24. Konstantinova, E.: J. Magn. Magn. Mater. **320**, 2721–2729 (2008)
25. Alonso, J.J., Fernandez, J.F.: Phys. Rev. B **74**, 184416 (2006)
26. Wieser, R., Nowak, U., Usadel, K.D.: Phys. Rev. B **69**, 064401 (2004)
27. Wysin, G.M., Pereira, A.R., Marques, I.A., Leonel, S.A., Coura, P.Z.: Phys. Rev. B **72**, 076533 (2005)